Foams Stabilized by In-Situ Surface-Activated Nanoparticles in Bulk and Porous Media

Robin Singh and **Kishore K. Mohanty,** University of Texas at Austin

Summary

Foams for subsurface applications are traditionally stabilized by surfactants. The goal of this work is to study foam stabilization by nanoparticles—in particular, by in-situ surface-hydrophobization of hydrophilic nanoparticles. The interfacial properties of the nanoparticles were modulated by the attachment of short-chain surface modifiers (alkyl gallates) that render them partially hydrophobic, but still fully dispersible in water. First, static foams were generated with nanoparticles with varying concentrations of surface modifiers. The decay of foam height with time was measured, and half-lives were determined. Optical micrographs of foam stabilized by surface-modified nanoparticles (SMNPs) and surfactant were recorded. Second, aqueous foams were created in-situ by coinjecting the SMNP solutions with nitrogen gas through a Berea sandstone core at a fixed quality. Pressure drop across the core was measured to estimate the achieved resistance factor. These pressure-drop results were then compared with those of a typical surfactant (alpha olefin sulfonate, alkyl polyglucoside) under similar conditions. Finally, oil-displacement experiments were conducted in Berea cores with surfactant and SMNP solutions as foaming agents (coinjection with nitrogen gas). A Bartsch shake test revealed the strong foaming tendency of SMNPs even with a very low initial surface-modifier concentration (0.05 wt%), whereas hydrophilic nanoparticles alone could not stabilize foam. The bubble texture of foam stabilized by SMNPs was finer than that with surfactants, indicating a stronger foam. As the degree of surface coating increased, the resistance factor of SMNP foam in a Berea core increased significantly. The corefloods in the sandstone cores with a reservoir crude oil showed that immiscible foams with SMNP solution can recover a significant amount of oil (20.6% of original oil in place) over waterfloods.

Introduction

With surging global energy demand and consumption, the existing oil reserves need to be exploited efficiently. Pressure depletion (primary), waterflooding, and gas drainage (secondary) are the common techniques used to recover oil, but more than half of the original oil is still left behind in reservoirs (Mohanty 2003). Enhanced-oil-recovery (EOR) techniques such as miscible gas injection, chemical flooding, and thermal recovery are being developed to recover the residual oil. Gasflooding is one of the most accepted and widely applied EOR methods (Orr 2007). It involves injecting hydrocarbon components such as methane, propane and enriched-gases, and nonhydrocarbon components [i.e., carbon dioxide (primarily), nitrogen, and flue gas] into oil reservoirs that are waterflooded. CO_2 flooding is now environmentally and economically feasible because of current high oil prices and the availability of large amounts of CO_2 from massive natural CO_2 sources, large anthropogenic sources such as gas-processing plants that remove CO_2 from natural gas, and emerging sources from chemical-manufacturing facilities (Enick et al. 2012). In principle, gasflooding is effective in improving microscopic sweep efficiency (Lake 1989). In fact, if the gas is first-contact or multicontact miscible with the oil, it can displace virtually all the oil in the volume swept by the gas (Orr et al. 1982). However, the volumetric sweep efficiency of gasflood is often very poor because of reservoir heterogeneity, gravity segregation, and viscous instability (Rossen et al. 2010).

Foam is a potential solution to the technical challenges associated with gas-injection processes (Kovscek et al. 1994; Rossen et al. 2010; Haugen et al. 2010). It can dramatically reduce gas mobility by several orders of magnitude by increasing the apparent viscosity of gas and trapping a large gas fraction inside the porous medium (Bernard and Jacobs 1965; Hirasaki and Lawson 1985). Conventionally, surfactants were used to stabilize foam lamellae in the porous media in which continuous regeneration of these lamellae is an essential mechanism for foam transport (Rossen 1996; Chen et al. 2010; Roostapour and Kam 2013). The quantity of surfactant required for long-distance propagation of foam from the wellbore is the key factor governing the cost associated with surfactant-stabilized foam (Kibodeaux and Rossen 1997). Various factors such as surface adsorption, surfactant loss caused by partitioning into crude oil, and surfactant degradation under harsh reservoir conditions limit further the economic viability of surfactant usage in subsurface applications (Grigg and Mikhalin 2007; Chen et al. 2012). The use of nanoparticles can help mitigate these issues. Nanoparticle-stabilized foam/emulsion recently has been of interest in the petroleum industry because of its potential to withstand harsh conditions of temperature and salinity. Moreover, recent advances in nanoparticle technology have allowed economical bulk production of nanoparticles from low-cost raw materials such as fly ash and silica. (Paul et al. 2007).

One can solely stabilize bulk foam with colloidal particles with various surface chemistries (Alargova et al. 2004; Binks and Horozov 2005; Gonzenbach et al. 2006). Most of these particles were coated with surfactants or polymers to act as surface-active agents because they were not amphiphilic themselves. Alargova et al. (2004) achieved superstabilized aqueous foams that retained constant volume for days with synthesized polymer microrods in the absence of surfactants. These foam bubbles were sterically stabilized by the entangled rod-shaped structures of the polymer. Espinosa et al. (2010) demonstrated very stable supercritical CO_2-in-water (C/W) foam generation in beadpacks with hydrophilic silica nanoparticles coated with polyethylene glycol (PEG). However, Worthen et al. (2012) showed that foams generated with partially hydrophobic silica nanoparticles in beadpacks were more stable than those with PEG-coated silica nanoparticles. Yu et al. (2014) investigated the effect of silica-nanoparticle structure and hydrophobicity on supercritical CO_2 foam behavior in glass beadpacks. The CO_2 bubble size decreased significantly with an increase in the hydrophobicity of silica nanoparticles. Mo et al. (2014) reported the effect of pressure, temperature, and rock samples on the performance of nanoparticle-stabilized CO_2 foam on residual oil recovery. The recovery over waterflood increased with the increase in pressure and decreased with the increase in temperature. Nguyen et al. (2014) studied C/W foams stabilized by partially hydrophobic silica nanoparticles in a microfluidic device. They observed a better sweep efficiency and smaller emulsion sizes in the case of nanoparticle foamflooding compared with CO_2 flooding. In summary, one can use surface-modified

This paper (SPE 170942) was accepted for presentation at the SPE Annual Technical Conference and Exhibition, Amsterdam, 27–29 October 2014, and revised for publication. Original manuscript received for review 23 July 2014. Revised manuscript received for review 1 February 2015. Paper peer approved 12 February 2015.

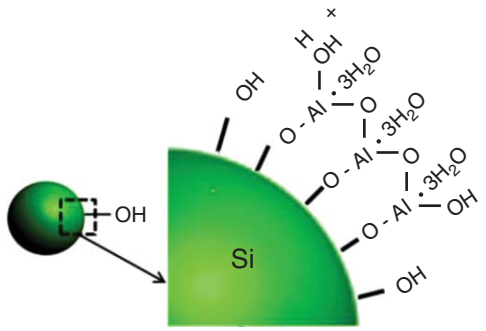

Fig. 1—Sketch of alumina-coated silica nanoparticle.

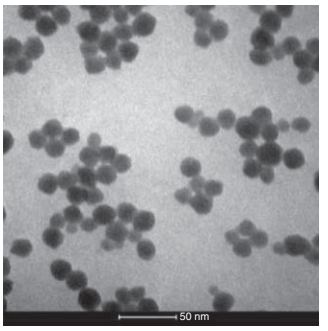

Fig. 2—TEM image of Ludox nanoparticles (scale bar is 50 nm).

nanoparticles (SMNPs) to stabilize foam, and several researchers investigated these SMNPs as foam stabilizers in both bulk and porous media.

Kam and Rossen (1999) theoretically demonstrated that one can use solid particles to stabilize foam without the presence of surfactants. Binks and Horozov (2005) tuned the contact angle of the silica nanoparticles quantitatively by varying the degree of controlled silanization. They were the first to experimentally report stable aqueous foams stabilized solely by silica nanoparticles with different degrees of hydrophobicity. Since then, several publications explored such systems in detail (Martinez et al. 2008; Stocco et al. 2009, 2011). However, this technique is not versatile. It is restricted exclusively to silica nanoparticles because only they can provide abundant silanol groups that facilitate surface modification by means of silane treatment (Cui et al. 2013). Moreover, surface modification of nanoparticles by means of chemical treatment tends to be expensive. In such cases, altering the surface property of particles by in-situ physioadsorption, chemisorption of surfactants, or adsorption of amphiphiles on their surfaces could be cost-effective.

Surface modification of nanoparticles by means of physiochemical interactions with surfactants was shown to be a facile route for foam stabilization. Several researchers have investigated the potential of using the synergy between surfactant and nanoparticles to generate foam. Singh and Mohanty (2014) investigated the synergistic stabilization of foam with a mixture of surface-modified nanoparticles and anionic surfactant in the Berea sandstone cores. They demonstrated that, by adding a small amount of nanoparticles to the surfactant solutions, foam stability dramatically increased, which was evident from the high resistance factor (RF) achieved in their foam-flow experiments. Worthen et al. (2013) reported the generation of viscous and stable C/W foams with fine texture by use of bare silica nanoparticles and zwitterionic surfactant in beadpacks, when neither of these species could stabilize foam independently. Cui et al. (2010) showed that one can surface activate nonsurface-active $CaCO_3$ nanoparticles by means of interaction with anionic surfactants, leading to enhanced foamability in bulk. The electrostatic interaction between the positive charges on particle surfaces and the negative charges of anionic surfactant headgroups results in the monolayer adsorption of the surfactant at the particle/water interface.

In-situ surface activation of nanoparticles by adsorption of short-chain amphiphiles was demonstrated as an effective method for foam stabilization in the bulk. Gonzenbach et al. (2006) demonstrated that one can partially hydrophobize inorganic colloidal particles with certain amphiphiles to produce ultrastable wet foams that could exhibit remarkable stability. Short-chain carboxylic acids, alkyl gallates, and alkylamines were used as amphiphiles that had the tendency to efficiently anchor on the particle surfaces. The unique colloidal architecture (i.e., the sequential assembly of amphiphiles on the surface of the particle and on the particle at the air/water interface) was the proposed mechanism for long-term stability of foam. Liu et al. (2009) used the same technique to obtain stable foams stabilized by hexylamine-modified laponite particles. They observed an increase in dilational viscoelasticity modulus with an increase in hexylamine concentration, which they attributed to one of the mechanisms for increased bubble stability in these systems.

The concept of in-situ hydrophobization of nanoparticles for foam stabilization has not yet been used in subsurface applications. On the basis of our review of the literature, previous studies focused on foam stabilized by either nanoparticles with different degrees of surface modification or by surfactant/nanoparticle mixtures, but not by in-situ surface-lyophobization of nanoparticles. The objective of this paper is to explore foam stabilization by means of in-situ surface activation of nanoparticles in bulk and porous media. We tailored the surface chemistry of the hydrophilic nanoparticles by adsorption of a small amount of short-chain surface modifiers (randomly on the surface) to obtain SMNPs. We then created foams in-situ by coinjecting an SMNP solution and nitrogen gas through Berea sandstone at a fixed quality, and measured the RF. The RF is defined as the ratio of the pressure drop across the core caused by coinjection of gas and SMNP/surfactant solution to the pressure drop caused by the coinjection of gas and brine at the same flow rate and quality. Finally, waterfloods and subsequent foamfloods were conducted in Berea cores saturated with a crude oil with SMNP solution and surfactant as foaming agents. This methodology and the results are described in the next sections.

Experiment	Porosity (%)	Permeability (md)	Initial Oil Saturation (%)
Foam flow	22	606	–
Coreflood 1	20	442	70
Coreflood 2	22	585	70
Coreflood 3	18	125	71.8

Table 1—Properties of the core used.

Methodology

Materials. Alumina-coated silica nanoparticles, Ludox CL, were supplied by Sigma-Aldrich. **Fig. 1** illustrates the surface configuration of these nanoparticles, showing the core silica with alumina surface coating. The size of the nanoparticles was characterized with a transmission electron microscope (TEM). The FEI Tecnai TEM operated at 80kV. The mean diameters of the primary particles were measured to be 20 nm. A TEM image is shown in **Fig. 2.** Nonionic-surfactant Triton CG-110, an alkyl polyglucoside (60% active), and anionic-surfactant Bioterge AS-40, a $C_{14–16}$ alpha-olefin sulfonate (39% active), were obtained from Dow Chemical Company and Stepan Company, respectively. Ultrapure water with resistivity greater than 18.2 mΩ·cm was used to prepare brine solutions. Berea sandstone cores were used in foam-flow and oil-displacement experiments. The properties of the cores are tabulated in **Table 1.** Crude oil was obtained from a reservoir and had a viscosity of 30 cp at 25 °C and a gravity of 26.6 °API. Propyl gallate (PG) (Sigma-Aldrich), sodium chloride (99%, Fisher Chemical), and nitrogen (research grade, Matheson, USA) were used as received.

Preparation of Nanoparticle Dispersion. First, the stock solution of 5 wt% of Ludox CL nanoparticles was prepared with

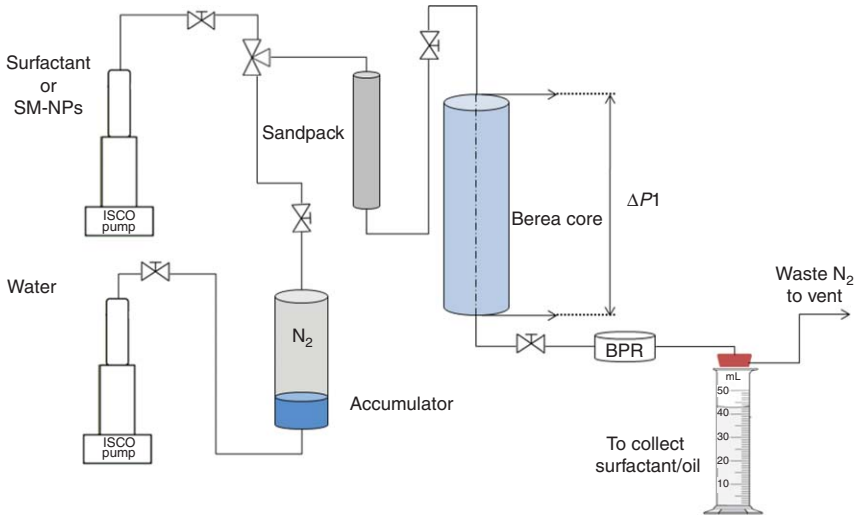

Fig. 3—Schematic of the apparatus for foam-flow experiments and corefloods.

ultrapure water. This stock solution was diluted to prepare samples. A surface modifier, PG, was added slowly to these samples with continuous magnetic stirring to avoid any local particle coagulation. Samples containing 1 wt% of nanoparticles with varying concentrations of PG (0.05 wt%, 0.075 wt%, and 0.1 wt%) were prepared. These samples were stirred for 48 hours to ensure mixture homogeneity and reaction equilibrium. The mixing was performed at room temperature at normal pH without any adjustment. With assuming a random monolayer attachment of the modifier on the surface and with using the nanoparticle dimension and the projection area of the modifier, the degree of surface coating was theoretically estimated to be 42.2, 63.3, and 84.4%, respectively, for these three cases. The zeta-potential and particle hydrodynamic diameters of these aqueous dispersions were characterized with the Delsa Nano analyzer.

Foamability and Static-Foam Tests. Preliminary foam tests were conducted by a Bartsch shake test in which 15 cm^3 of these samples was vigorously shaken 10 times in test tubes, and their macroscopic foam textures were observed. To observe the texture in detail, the bubble samples were placed on microscope slides, and the images were recorded with a Nikon microscope equipped with a high-resolution camera. Image J software was used to analyze these images and to determine bubble-size distribution. At room temperature, 20 cm^3 of each sample was then taken in a graduated cylinder (diameter of 1 cm, length of 20 cm). The apparatus consisted of a transparent cylinder made of acrylic with a stainless-steel sparging frit (pore size of 2 μm) at the bottom, which was used to disperse air. Both ends of the cylinder had Swagelok fittings that prevented evaporation. Air was injected from the bottom, generating static foam. The height of the foam (above the liquid phase) was monitored as a function of time.

Foam-Flow Experiments. Cylindrical cores with a 1- or 1.5-in. diameter and a 1-ft length were drilled from the block of Berea sandstone. Berea is an oil-free outcrop rock; thus, no precleaning was required. The cores were dried at 90 °C for 24 hours in an oven and laminated with FEP shrinkwrap tubing (Geophysical Supply Company, Houston). These cores were then placed in a Hassler-type coreholder (Phoenix, Houston, USA) with a confining pressure of 1,500 psi. The petrophysical properties of the cores, such as air porosity and permeability, were then determined. **Fig. 3** shows the experimental schematic. Two Series-D syringe pumps from Teledyne Isco (Lincoln, Nebraska, USA) capable of low injection rates (as low as 0.001 cm^3/min) were used in the setup. The apparatus was built to coinject nitrogen gas and a surface-modified-nanoparticle (SMNP) solution through a sandpack (0.6-in. diameter and 6-in. length) to ensure proper mixing and foam generation. The pregenerated foam was then injected at the top of the core. The downstream pressure of the experiment was maintained by a backpressure regulator (Equilibar, North Carolina, USA) installed after the coreholder. The pressure drops across the core were measured with Rosemount differential-pressure transducers. All connections were made with stainless-steel Swagelok fittings.

Oil-Displacement Experiments. Coreflood experiments investigated the foam behavior of the SMNP solution in the presence of crude oil in comparison to that with a surfactant. The objective was to study the foam rheology and microscopic sweep efficiency of foam. Because the cores used in these experiments were 1 in. in diameter and were quite homogeneous, volumetric sweep-efficiency improvement was not an important factor here. The experimental setup was similar to that described in Fig. 3. First, the brine porosity and permeability of the cores were determined. Second, the cores, fully saturated with brine, were then flooded with filtered crude oil [at least 2.5 pore volumes (PV)] from the top at a constant pressure of 750 psi at room temperature until no brine was produced. Third, the initial oil saturation was determined by mass balance. Fourth, the whole setup was pressurized with a backpressure of 100 psi. The brine flood was conducted at 1ft/D for 2 PV until no oil was produced. Then, the core was flooded with brine at 5 ft/D to minimize capillary end effects. The cores were then preflushed with 1 PV of surfactant or SMNP solution to avoid any adsorption of surfactant while foamflooding. Nitrogen gas and either surfactant or an SMNP solution were then coinjected through sandpack. This pregenerated foam was then injected into the core from the top for more than 7 PV. Oil recovery and pressure drops were monitored at each step.

Results and Discussion

Surface Hydrophobization of Nanoparticles. In a surfactant-free system, particle adsorption at the air/water interface is a necessary condition for foam stabilization solely by particles. Foam stability is governed mainly by the interfacial property of the particle—the contact angle (θ). In their experimental work, Binks and Horozov (2005) showed that highly hydrophilic and highly hydrophobic particles tend to destabilize foam. Thus, proper tuning of the contact angle of particles is required to obtain stable foam. Therefore, our first objective was to make the nanoparticle surface partially hydrophobic. This was achieved by anchoring a short-chain surface modifier, propyl gallate (PG), to the particle surface. The surface of the nanoparticle is covered primarily by $-OH_2^+$ groups, which are the potential sites for a surface-modifier attachment. The positive zeta-potential of these nanoparticles confirms the presence of these $-OH_2^+$ groups. PG, which has multiple

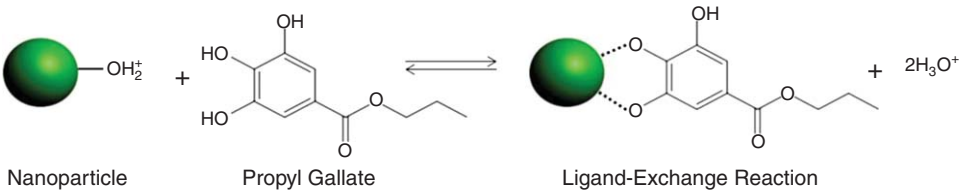

Fig. 4—Ligand-exchange reaction between nanoparticle and PG.

Nanoparticle Concentration (wt%)	Surface-Modifier Concentration (wt%)	Zeta-Potential of SM-NPs (mV)
1	0	32.84
1	0.05	23.78
1	0.075	17.14
1	0.1	13.39

Table 2—Zeta-potential of the SM-NPs with different initial surface-modifier concentration.

hydroxyl groups, can attach to these $-OH_2^+$ groups by means of ligand-exchange reactions. After this reaction, the $-OH_2^+$ groups on the particle surface are replaced by hydroxyl groups of PGs, as shown in **Fig. 4.**

Note that the attachment by means of ligand-exchange reactions is stronger than mere electrostatic interactions between oppositely charged particles and functional groups of modifiers (Hidber et al. 1997). This attachment reaction is also independent of the charge of the nanoparticles, and it can occur even if the particle surface is negatively charged at a different pH (Gonzenbach et al. 2006). The reduction in zeta-potential of surface-modified-nanoparticles (SMNP) solutions with the increase in surface-modifier concentration confirmed the attachment reaction, as shown in **Table 2.**

Foamability and Bubble Texture. Preliminary foam tests were conducted by shaking 15-cm^3 samples vigorously for ten times in test tubes and by observing the macroscopic foam textures. **Fig. 5** shows the resulting foam for $t = 0$ minutes, 30 minutes, and 240 minutes. Sample A had 1 wt% of nanoparticles, Sample B had 0.05 wt% PG, and Sample C had a mixture of 1 wt% nanoparticles and 0.05 wt% PG that was stirred magnetically for 24 hours. Sample A did not show any foaming tendency, because it had only hydrophilic nanoparticles. Sample B showed some initial foaming, but the foam collapsed in a few minutes. However, Sample C formed a strong foam with fine texture that remained stable for a long time ($t > 240$ minutes). This basic foam test confirmed that foam stabilized solely by nanoparticles is possible if the surface of the nanoparticle is partially hydrophobic.

Fig. 6 (top) shows the optical micrographs of the foam stabilized by different cases. Quantitative analysis of these images was performed with the corresponding threshold images, as shown in Fig. 6 (bottom), to estimate average bubble radius, Ravg. A non-ionic surfactant, Triton CG-100, which is a good foaming agent (Rafati et al. 2012), was used as a base case to compare the foam texture of the SMNP-stabilized foam. Large bubbles were observed for the case of the surfactant (Fig. 6A) in which the Ravg was found to be 84 μm. Figs. 6b, 6c, and 6d show the texture of foam stabilized by SMNPs with initial surface-modifier concentrations of 0.05, 0.075, and 0.1 wt%, respectively. Relatively finer bubbles were observed for these three cases, and Ravg was calculated to be 51, 32, and 38 μm, respectively. Smaller bubbles indicate a stronger foam, which was the result of the retarded coalescence of bubbles caused by the adsorption of SMNPs on the air/water interface.

Static-Foam Test. Static foam tests were conducted with SMNPs with varying concentrations of the initial surface-modifier concentration. The decay of foam height was monitored over time. These tests were conducted at room temperature. **Fig. 7** shows the plot of relative foam height vs. decay time in hours. One can determine the half-life, which is the time it takes for the foam to decay to half its original height, from the plot. The half-life of the foam for SMNPs with an initial modifier concentration of 0.05, 0.075, and 0.1 wt% was found to be 11, 23, and 34 hours, respectively. The large magnitude of the half-lives indicates stable foam formation stabilized by SMNPs. As the concentration of the surface modifier increased, the half-lives increased significantly, suggesting an increased affinity of SMNPs to the air/water interface. The macroscopic foam textures observed (by the naked eye) in these three cases were quite similar and were characterized by very fine bubbles. Fig. 7 shows the foam morphology for the case of SMNPs with a 0.1-wt% surface-modifier concentration.

Mechanisms for Foam Stabilized Solely by SMNPs. The key mechanisms responsible for foam stabilization by a nanoparticle system such as particle-detachment energy, maximum capillary pressure of coalescence, and kinetics of film drainage are explained in detail in our previous study (Singh and Mohanty 2015). In this paper, we focus on the concept of in-situ hydrophobization of nanoparticles for foam stabilization. The term "in-

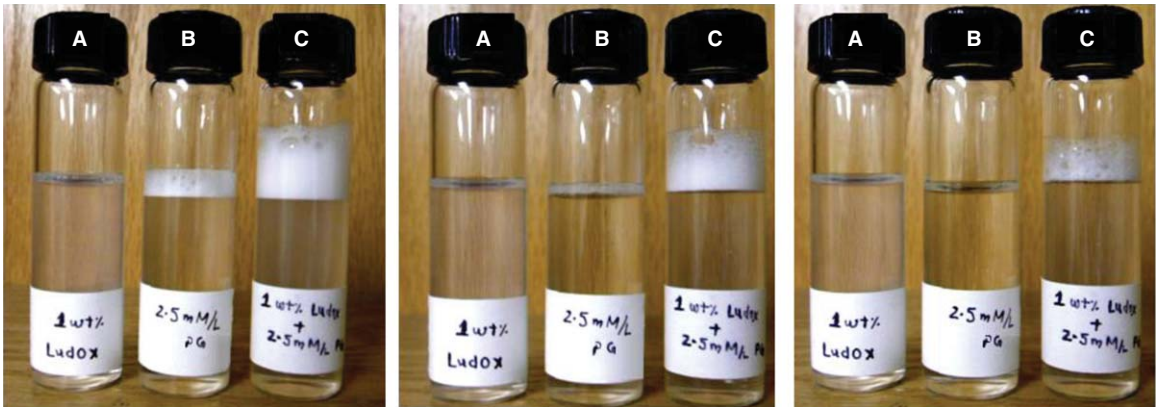

Fig. 5—Foamability at three different times (a) 1 wt% NP, (b) 0.05 wt% PG, (c) 1 wt% NP + 0.05 wt% PG.

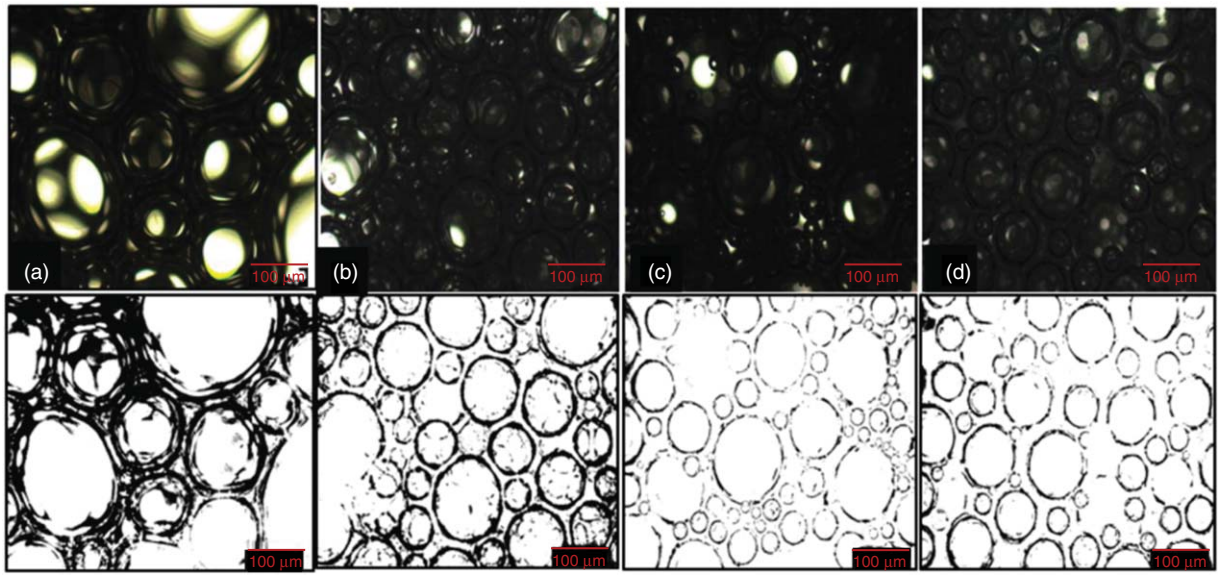

Fig. 6—Optical micrographs of foam stabilized by (a) 0.5 wt% Triton CG-100, (b) 1 wt% NP + 0.05 wt% PG, (c) 1 wt% NP + 0.075 wt% PG, and (d) 1 wt% NP + 0.1 wt% PG (scale bar is 100 μm) before (top panels) and after (bottom panels) image processing.

situ" here refers to "in the localized reaction mixture," which is commonly used in chemistry literature and does not imply "inside the porous medium." This technique relies on the selection of a suitable surface modifier that can attach itself to the nanoparticle surface by means of either electrostatic interaction or ligand-exchange reaction. The surface modifier requires hydrophilic groups that can attach to the hydrophilic nanoparticle surface and short-chain hydrophobic groups that can render the surface partially hydrophobic. The short chain ensures the high solubility of surface modifiers in the water and prevents phase separation. In this work, the degree of surface modification of nanoparticles was controlled by varying the concentration of the surface modifier (0.05, 0.075, and 0.1 wt%) while keeping the nanoparticle concentration constant at 1 wt%. With assuming a random monolayer attachment of the modifier on the surface and with using the nanoparticle dimension and the projection area of the modifier, the degree of surface coating was theoretically estimated to be 42.2, 63.3, and 84.4%, respectively, for these three cases. The modified nanoparticles were characterized with the Delsa Nano analyzer. No increments in nanoparticle diameters were observed in these samples compared with the unmodified-nanoparticle sample, indicating no aggregation and a strong aqueous stability. The particle-detachment energy, E, which is the amount of energy required to move the particle from the interface to the bulk solution is given by

$$E = \pi R^2 \gamma_{aw}(1 - |\cos\theta|)^2, \quad \ldots\ldots\ldots\ldots\ldots\ldots\ldots\ldots (1)$$

where R is the particle radius, γ_{aw} is the surface tension of the interface, and θ is the contact angle. The detailed derivation is reported by Binks and Lumsdon (2000). The contact-angle determination is quite difficult experimentally; however, one can perform a qualitative analysis of energy on the basis of the equation. The nanoparticles used in this work are inherently highly hydrophilic (θ close to zero). Thus, they did not show any affinity toward the air/water interface, and E is quite low (for the case of $R = 10$ nm and $\gamma_{aw} = 72$ dyne/cm), as shown in **Fig. 8** (left). However, surface modification by anchoring modifiers on the surface rendered them partially hydrophobic. The obtained SMNPs had a positive affinity toward the air/water interface and were able to stabilize foam as observed experimentally in foam-shake tests. The detachment energy also increases significantly—on the order of 1,000. Fig. 8 (right) illustrates this mechanism, showing air bubbles stabilized by nanoparticles (green spheres) that are coated with modifiers (black molecules).

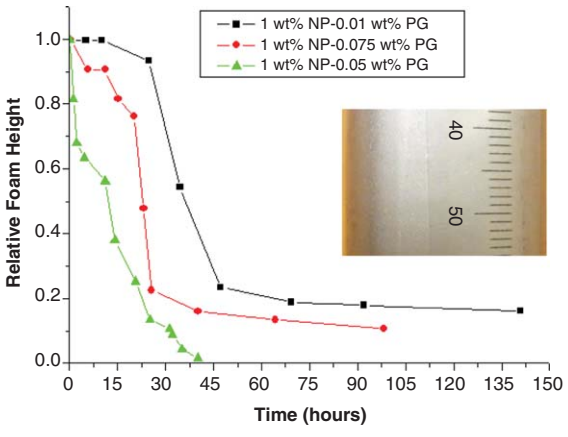

Fig. 7—Static foam tests of different samples. The inset picture shows the morphology of foam stabilized by SMNPs with 0.1 wt% surface-modifier concentration.

Foam-Flow Experiments. Foam-flow experiments were conducted in Berea sandstone core with a 1.5-in. diameter and 1-ft length by use of SMNPs with different degrees of surface coating as the foaming agent. The brine porosity and permeability of the core were 22% and 606 md, respectively. The flow rates in these experiments were maintained at 4 ft/D. This was performed to achieve a sufficient pressure drop that one can measure accurately. All these experiments were performed at room temperature and with a backpressure of 100 psi. Before each run, the SMNP-solution preflush was conducted to saturate the core with SMNPs and to avoid any modifier-adsorption issues while foamflooding. After the SMNP-solution preflush [1 pore volume (PV)], nitrogen gas and the SMNP solution were coinjected into the sandpack to generate foam at 4 ft/D and with a quality of 90%. This pregenerated foam was injected from the top of the core for at least 3.5 PV to achieve a steady-state pressure drop. During the foam-generation step in porous media, lamellae are created by the snapoff process. This process is driven by bulk flow at pore throats; a thick lamella is first formed that later drains down to a thin lamella. The number density of nanoparticles in the liquid phase (with a nanoparticle concentration of approximately 0.1 to 0.5 wt%) is quite

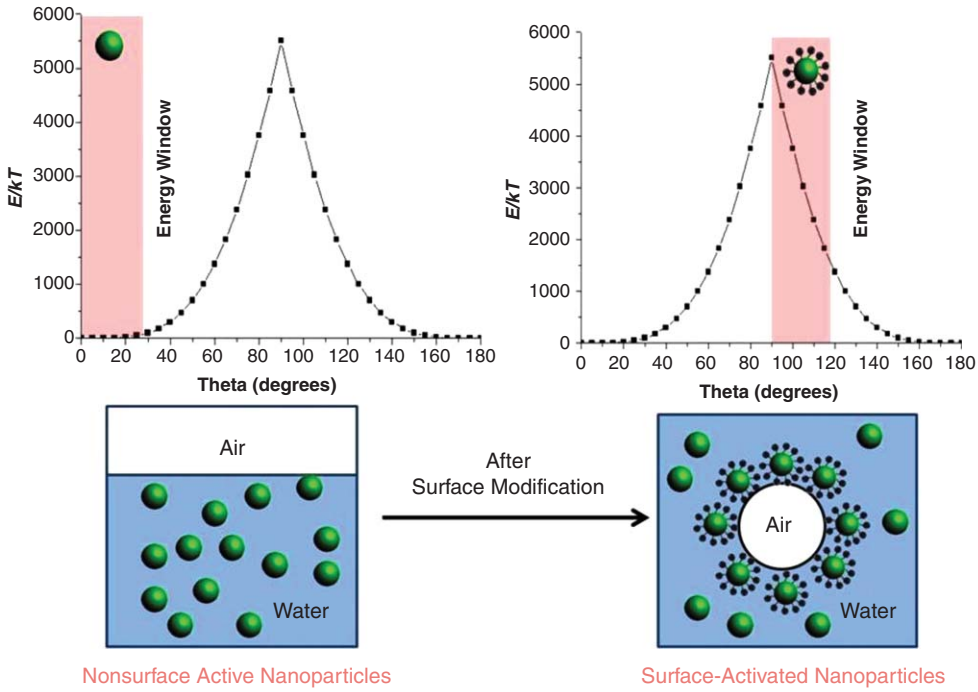

Fig. 8—Mechanism of foam stabilization.

high. The nanoparticles are part of this film from the inception of snapoff and do not have to diffuse into it. Thus, one can create foam by coinjecting the nanoparticle dispersion and nitrogen into a porous medium simultaneously. After completing each run, the core was cleaned by flushing more than 15 PV of brine. The back-pressure was intermittently depressurized and pressurized several times to remove the trapped gas. We ensured that the brine-flow pressure drop was approximately the same as the initial single-phase brine pressure drop.

First, the base case was conducted in which brine and nitrogen gas were coinjected at 4 ft/D with a quality of 90%. **Fig. 9** (left) shows the pressure-drop profile for the base case. The pressure drop showed some fluctuations, but the average pressure drop in the steady state was 0.8 psi, which is quite low. This run was then repeated with brine containing 1 wt% of unmodified nanoparticles. The pressure drop in this case was also approximately 0.8 psi, indicating no foaming tendency of unmodified nanoparticles even in the porous medium. In the subsequent runs, SMNPs were used as foaming agents with different degrees of surface coating. Fig. 9 (right) shows the case of SMNPs with an initial surface-modifier concentration of 0.05 wt%, which is equivalent to 42.2% surface coating. The average pressure drop in the steady state in this case was approximately 3.2 psi, which was four times the base case. This additional pressure drop over the base case indicated the formation of in-situ foam. The core was then cleaned by following the aforementioned steps. **Fig. 10** shows the pressure-drop profile for the case of SMNPs with an initial surface-modifier concentration of 0.075 wt% (equivalent to 63.3% surface coating) (left) and 0.1 wt% (equivalent to 84.4% surface coating) (right). The average steady-state pressure drop after 3.5 PV of coinjection was found to be 6.1 and 11.7 psi, respectively. The large pressure drop achieved in these cases is a result of the finer in-situ bubble texture stabilized by partially hydrophobic SMNPs, as observed in the bulk foam-stability tests. For comparison, this experiment was repeated with a nonionic surfactant, Triton CG-100, as the foaming agent. The concentration of the surfactant was varied (0.02, 0.2, and 0.5 wt%). The average steady-state pressure drop was found to be 0.8, 2.6, and 13.6 psi, respectively. The resistance factor (RF) is defined (here) as the ratio of the pressure drop across the core caused by coinjection of gas and an SMNP/surfactant solution to the pressure drop caused by the coinjection of gas and brine at the same flow rate (4 ft/D) and quality (90%). **Fig. 11** compares the RF achieved in the porous medium for SMNPs with different surface coatings and a

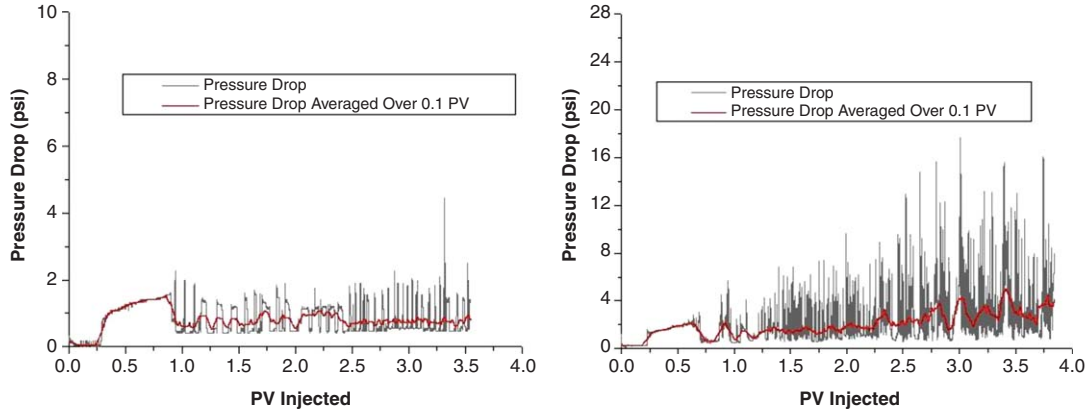

Fig. 9—Pressure-drop profile for the coinjection of nitrogen and sample at 4 ft/D with quality of 80%. Sample: Brine (left); 1 wt% NP-0.05 wt% PG (right).

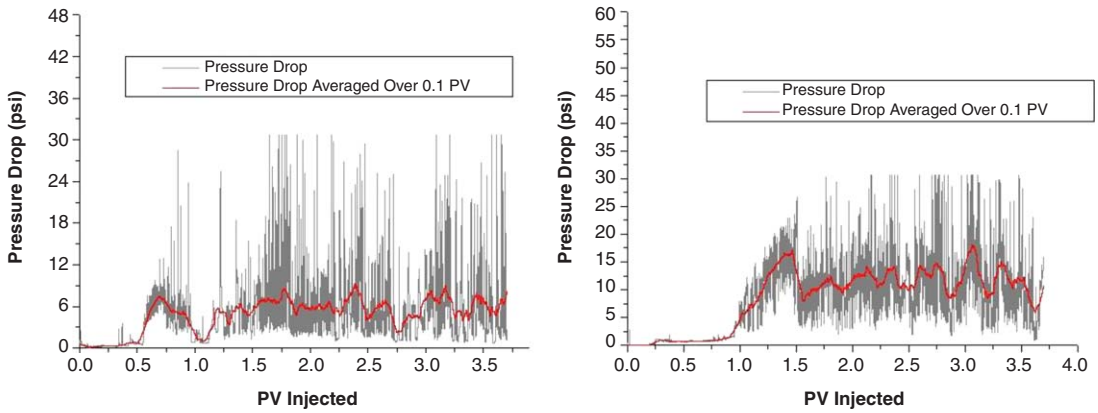

Fig. 10—Pressure-drop profile for the coinjection of nitrogen and sample at 4 ft/D with quality of 80%. Sample: 1 wt% NP/0.075 wt% PG (left); 1 wt% NP/0.1 wt% PG (right).

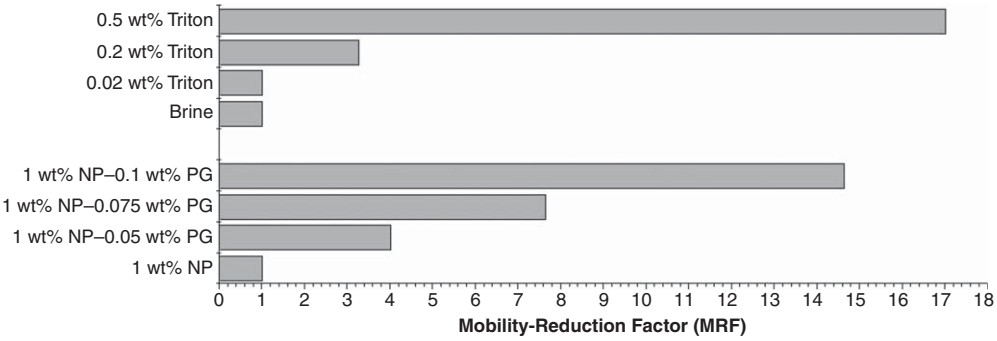

Fig. 11—Comparison of steady-state RF achieved for SMNP solutions and a nonionic surfactant.

surfactant at different concentrations. This plot indicates that SMNPs have the potential to behave as a surfactant and a promising foaming agent.

Oil-Displacement Experiments. Coreflood experiments evaluated foam rheology in the presence of residual crude oil and the microscopic sweep efficiency of the SMNP-stabilized foam in comparison to the surfactant-stabilized foam. Coreflood 1 was conducted in a Berea core with a dead crude oil and a surfactant. The core was 1 in. in diameter and 1 ft in length with 20% porosity and 442-md permeability. The initial oil saturation was 70%. **Fig. 12** shows the injection procedure, cumulative oil recovery (secondary *y*-axis), and overall pressure drop (primary *y*-axis) across the core. A brine flood was conducted at 1 ft/D to mimic waterfloods at a typical field rate and continued for approximately 2 PV until no oil was produced. The waterflood oil recovery was 50.2% of original oil in place (OOIP), and the oil saturation reduced to 34.8%. The pressure drop during the waterflood was between 2.1 and 2.6 psi. To minimize any capillary end effect, brine was then injected at 5 ft/D for another 1 PV. The pressure drop increased to 10.5 psi as the flow rate was increased fivefold. No oil was recovered during this stage, implying no significant capillary end effect. Before conducting the foamflood, the core was preflushed with 0.5 wt% of anionic surfactant, Bioterge AS-40, which is a good foaming agent (Spirov et al. 2012; Simjoo et al. 2013), for 1 PV at 1 ft/D to avoid any surfactant adsorption during foamflooding. No oil was recovered during surfactant

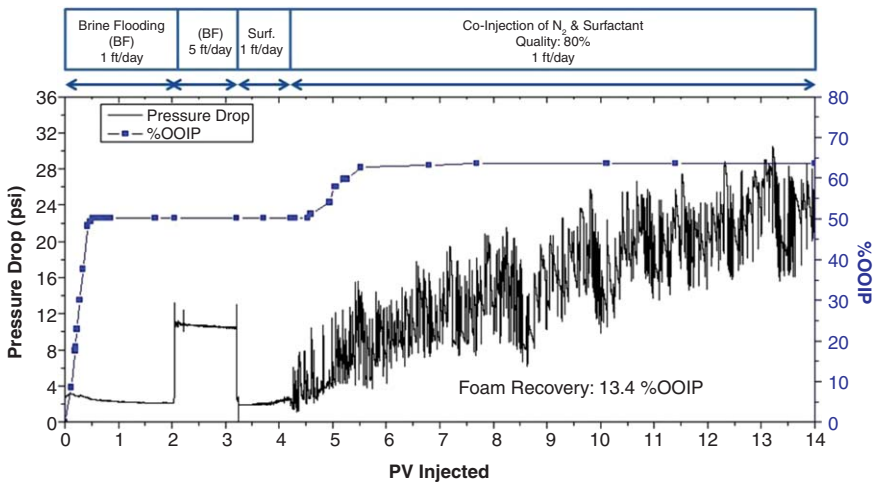

Fig. 12—Pressure-drop profile (left axis) and cumulative oil recovery (right axis) for Coreflood 1.

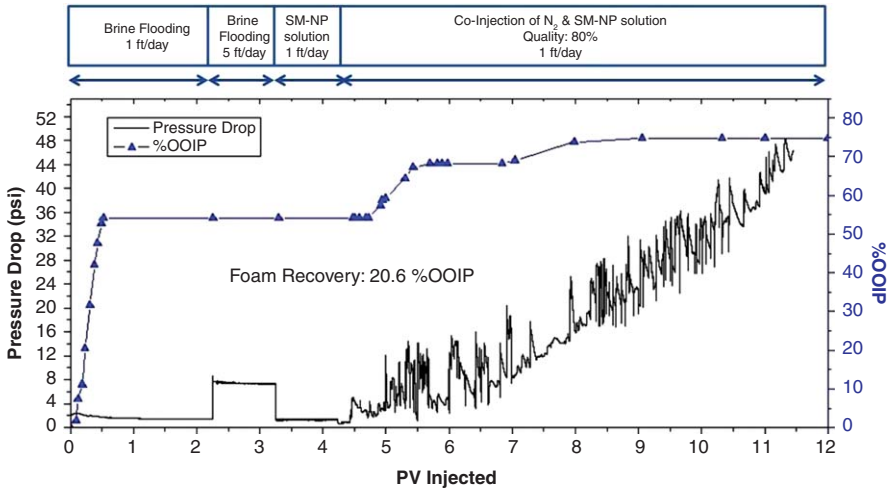

Fig. 13—Pressure-drop profile (left axis) and cumulative oil recovery (right axis) for Coreflood 2.

injection because the surfactant does not lower the interfacial tension sufficiently to mobilize residual oil. The pressure drop during preflush was approximately 2 psi. Then, a coinjection of 0.5 wt% of surfactant solution and nitrogen gas was started with a quality of 80% at 1ft/D. The additional oil recovery for the first 3.5 PV of coinjection over waterflood was 13.4% of OOIP. No significant amount of oil was produced after 3.5 PV of injection, but the coinjection was continued for another 3.5 PV to observe the foam rheology in the presence of residual oil. The average pressure drop continued to grow and reached 25.8 psi at the end of the experiment. The ultimate cumulative oil recovery was 63.6% of OOIP, and final oil saturation was 25.5%.

Coreflood 2 was then conducted in another Berea core with the same procedure as the previous coreflood, but with SMNPs as the foaming agent instead of the anionic surfactant. The core was 1 in. in diameter and 1 ft in length with a porosity and a permeability of 22% and 585 md, respectively. The initial oil saturation in this case was also 70%. The cumulative oil recovery (% OOIP) (secondary *y*-axis) and overall pressure drop (primary *y*-axis) are shown in **Fig. 13.** The core was flooded with brine for 2 PV at 1 ft/D, which represents a waterflood. The waterflood reduced the oil saturation to 32% and resulted in an oil recovery of 54.1% of OOIP. The pressure drop during this waterflood stage was between 1.4 and 2.2 psi. Then, the core was flooded with brine for 1 PV at 5 ft/D. No additional oil was recovered, implying a negligible capillary end effect. The pressure drop increased to approximately 7.4 psi at the flow rate of 5 ft/D. Next, the core was preflushed with an SMNP solution (1 wt% of nanoparticles modified by 0.1 wt% of surface modifiers) for 1 PV. No oil was recovered during this stage. Coinjection of an SMNP solution and nitrogen gas was then conducted at 1 ft/D with 80% quality. The additional oil recovery over waterflood after 3.5 PV of injection was 19.6% of OOIP. The coinjection was continued for another 4.5 PV. The pressure drop in this coreflood went to approximately 39.6 psi at the end of the experiment. The ultimate cumulative oil recovery was 74.7% OOIP, foam recovery over waterflood was 20.6% OOIP, and final oil saturation was reduced to 17.6%.

Coreflood 3 was then performed in another Berea core with the same injection procedure as Coreflood 2, but with a reduced concentration of SMNPs (0.5 wt% of nanoparticles modified by 0.05 wt% of surface modifiers). The core was 1 in. in diameter and 1 ft in length with a porosity and a permeability of 18% and 125 md, respectively. The initial oil saturation in this case was 71.8%. The cumulative oil recovery (secondary *y*-axis) and overall pressure drop (primary *y*-axis) are shown in **Fig. 14.** The pressure drop during waterflood at 1 and 5 ft/D was 4.8 and 23.7 psi, respectively, which was relatively higher than the previous cases because of the lower permeability of the core. The waterflood recovered 48.3% of OOIP. The core was then preflushed with 1 PV of the SMNP solution (0.5 wt% nanoparticles modified by 0.05 wt% of surface modifiers) at 1ft/D. No oil was recovered during this stage, and the pressure drop was 4.3 psi. Then, the SMNPs solution and nitrogen gas were coinjected at 1 ft/D with 80% quality for more than 7 PV. The additional oil recovery over waterflood after 3.5 PV of foam injection was 14.8% of OOIP. The pressure drop at the end of the experiment was 17.3 psi. The

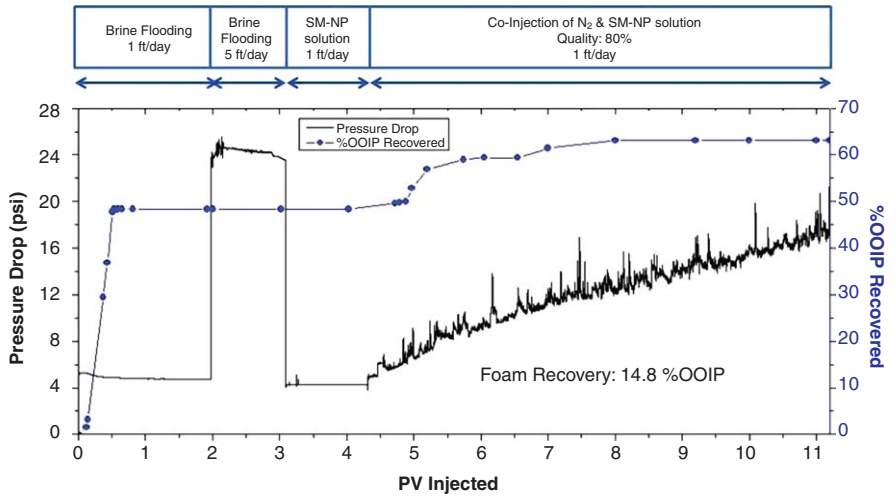

Fig. 14—Pressure-drop profile (left axis) and cumulative oil recovery (right axis) for Coreflood 3.

	Coreflood 1	Coreflood 2	Coreflood 3
Foaming agent	0.5 wt% anionic surfactant	1 wt% NP + 0.1% PG	0.5 wt% NP + 0.05 wt% PG
Steady-state pressure drop	25.8 psi	39.6 psi	17.3 psi
Foam recovery	13.4% of OOIP	20.6% OOIP	14.8% OOIP

Table 3—Comparison of the three corefloods.

ultimate cumulative oil recovery was 63.1% of OOIP; foam recovery over waterflood was 14.8% of OOIP; and final oil saturation was reduced to 26.5%.

Table 3 summarizes the results of the three oil-displacement experiments. These coreflood results reveal that immiscible foam can recover a significant amount of oil over waterflood. The oil recovery caused by SMNP-stabilized foam (20.6 and 14.8%) was greater than that by surfactant-stabilized foam (13.4%). This increase could be caused by stronger in-situ foam generation by the SMNP solution, resulting in better microscopic sweep efficiency compared with the surfactant.

This work is an initial study with SMNPs and is conducted under simplistic conditions. Preliminary experiments in bulk and porous media show that SMNPs could potentially generate foam in the absence of surfactant. However, the dynamics of these SMNPs in porous media for in-situ foam generation is still unknown. For these SMNPs to be a feasible foaming agent in subsurface applications, they should not adsorb or filter out in the porous media. Thus, retention and adsorption studies of SMNPs and surface modifier, respectively, are vital. Nanoparticles used in the present study are weakly positively-charged such that could adsorb on the negatively-charged sandstones. Future studies could use negatively-charged silica nanoparticles to reduce the adsorption of SMNPs. The concept of in-situ surface activation relies on the attachment of the surface modifier to the nanoparticle surface. Therefore, one also should investigate chromatographic separation of the surface modifier and nanoparticles on the surface of the porous medium.

Conclusions

Surface-modified nanoparticles (SMNPs) were obtained by partial hydrophobization of alumina-coated silica nanoparticles with a surface modifier. Foams were then stabilized by these SMNPs, which had a tendency to adsorb at the air/water interface, in both bulk and porous media in the absence of surfactants. One can draw the following conclusions from this work:

- The attachment of the surface modifier on the nanoparticle surface occurred because of ligand-exchange reactions that are stronger than electrostatic interactions. This prevented the detachment of these anchored groups from the surface during flow through porous media. This approach of tailoring the interfacial properties of the nanoparticles is quite simple and robust and does not require cumbersome chemical treatment, as opposed to surface modification by means of controlled silanization.
- A Bartsch shake test revealed the strong foaming tendency of SMNPs even with a very low initial surface-modifier concentration (0.05 wt%), whereas hydrophilic nanoparticles alone could not stabilize foam. The irreversible adsorption of such partially hydrophobic nanoparticles on the air/water interface results in foam stability.
- The optical micrographs showed that the bubble texture of foam stabilized by SMNP solutions was finer than that obtained by a typical surfactant.
- As the degree of surface coating increased, the resistance factor of SMNP foam in a Berea sandstone core increased significantly. These foam-flow experiments showed that one can stabilize foam in the porous medium by in-situ surface-activated nanoparticles, and that they have the potential to behave as a surfactant.
- Corefloods in a sandstone core with a reservoir crude oil showed that immiscible foams with SMNPs can recover a significant amount of oil over waterflood. These recoveries were comparable to or higher than those obtained when a surfactant was used as the foaming agent.

Acknowledgments

We are thankful to the sponsors of the Gas EOR Industrial Affiliates Project at the University of Texas at Austin and Statoil for partial funding this work. We would also like to thank Eric Dao for assisting us with the experimental work.

References

Alargova, R. G., Warhadpande, D. S., Paunov, V. N. et al. 2004. Foam Superstabilization by Polymer Microrods. *Langmuir* **20** (24): 10371–10374. http://dx.doi.org/10.1021/la048647a.

Bernard, G. G. and Jacobs, W. L. 1965. Effect of Foam on Trapped Gas Saturation and on Permeability of Porous Media to Water. *SPE J.* **5** (4): 295–300. SPE-1204-PA. http://dx.doi.org/10.2118/1204-PA.

Binks, B. P. and Horozov, T. S. 2005. Aqueous Foams Stabilized Solely by Silica Nanoparticles. *Angewandte Chemie* **44** (24): 3722–3725. http://dx.doi.org/10.1002/anie.200462470.

Binks, B. P. and Lumsdon, S. O. 2000. Influence of Particle Wettability on the Type and Stability of Surfactant-Free Emulsions. *Langmuir* **16** (23): 8622–8631. http://dx.doi.org/10.1021/la000189s.

Chen, Y., Ehlag, A. S., Poon, B. M. et al. 2012. Ethoxylated Cationic Surfactants for CO2 EOR in High Temperature, High Salinity Reservoirs. *Proc.*, SPE Improved Oil Recovery Symposium, Tulsa, Oklahoma, USA, 14–18 April. SPE-154222-MS. http://dx.doi.org/10.2118/154222-MS.

Chen, Q., Gerritsen, M. G., and Kovscek, A. R. 2010. Modeling Foam Displacemnet With the Local-Equilibrium Approximation: Theory and Experimental Verification. *SPE J.* **15** (1): 171–183. SPE-116735-PA. http://dx.doi.org/10.2118/116735-PA.

Cui, Z. G., Cui, Y. Z., Cui, C. F. et al. 2010. Aqueous Foams Stabilized by In-Situ Surface Activation of $CaCO_3$ Nanoparticles Via Adsorption of Anionic Surfactant. *Langmuir* **26** (15): 12567–12574. http://dx.doi.org/10.1021/la1016559.

Cui, H., Zhao, Y., Ren, W. et al. 2013. Aqueous Foams Stabilized Solely by CoOOH Nanoparticles and the Resulting Construction of Hierarchically Hollow Structure. *J. Nanoparticle Research* **15** (8): 1–7. http://dx.doi.org/10.1007/s11051-013-1851-7.

Enick, R., Olsen, D., Ammer, J. et al. 2012. Mobility and Conformance Control for CO2 EOR via Thickeners, Foams, and Gels—A Literature Review of 40 Years of Research and Pilot Tests. *Proc.*, SPE Improved Oil Recovery Symposium, Tulsa, Oklahoma, USA, 14–18 April. SPE-154122-MS. http://dx.doi.org/10.2118/154122-MS.

Espinosa, D., Caldelas, F., Johnston, K. et al. 2010. Nanoparticle-Stabilized Supercritical CO2 Foams for Potential Mobility Control Applications. *Proc.*, SPE Improved Oil Recovery Symposium, Tulsa, Oklahoma, USA, 24–28 April. SPE-129925-MS. http://dx.doi.org/10.2118/129925-MS.

Gonzenbach, U. T., Studart, A. R., Tervoort, E. et al. 2006. Stabilization of Foams With Inorganic Colloidal Particles. *Langmuir* **22** (26): 10983–10988. http://dx.doi.org/10.1021/la061825a.

Grigg, R. B. and Mikhalin, A. A. 2007. Effects of Flow Conditions and Surfactant Availability on Adsorption. *Proc.*, International Symposium on Oilfield Chemistry, Houston, Texas, USA, 28 February–2 March. SPE-106205-MS. http://dx.doi.org/10.2118/106205-MS.

Haugen, A., Ferno, M.A., Graue, A. et al. 2010. Experimental Study of Foam Flow in Fractured Oil-Wet Limestone for Enhanced Oil Recovery. *Proc.*, SPE Improved Oil Recovery Symposium, Tulsa, Oklahoma, USA, 24–28 April. SPE-129763-MS. http://dx.doi.org/10.2118/129763-MS.

Hidber, P. C., Graule, T. J., and Gauckler, L. J. 1997. Influence of the Dispersant Structure on Properties of Electrostatically Stabilized Aqueous

Alumina Suspensions. *J. European Ceramic Society* **17** (2): 239–249. http://dx.doi.org/10.1016/S0955-2219(96)00151-3.

Hirasaki, G. J. and Lawson, J. B. 1985. Mechanisms of Foam Flow in Porous Media: Apparent Viscosity in Smooth Capillaries. *SPE J.* **25** (2): 176–190. SPE-12129-PA. http://dx.doi.org/10.2118/12129-PA.

Kam, S. I. and Rossen, W. R. 1999. Anomalous Capillary Pressure, Stress, and Stability of Solids-Coated Bubbles. *J. Colloid and Interface Science* **213** (2): 329–339. http://dx.doi.org/10.1006/jcis.1999.6107.

Kibodeaux, K. R. and Rossen, W. R. 1997. Coreflood Study of Surfactant-Alternating-Gas Foam Processes: Implications for Field Design. *Proc.*, SPE Western Regional Meeting, Long Beach, California, USA, 25–27 June. SPE-38318-MS. http://dx.doi.org/10.2118/38318-MS.

Kovscek, A. R., Patzek, T. W., and Radke, C. J. 1994. Mechanistic Prediction of Foam Displacement in Multidimensions: A Population Balance Approach. *Proc.*, SPE Improved Oil Recovery Symposium, Tulsa, Oklahoma, USA, 17–20 April. SPE-27789-MS. http://dx.doi.org/10.2118/27789-MS.

Lake, L. W. 1989. *Enhanced Oil Recovery*. Upper Saddle River, New Jersey: Prentice Hall.

Liu, Q., Zhang, S., Sun, D. et al. 2009. Aqueous Foams Stabilized by Hexylamine-Modified Laponite Particles. *Colloids and Surfaces A: Physicochemical and Engineering Aspects* **338** (1): 40–46. http://dx.doi.org/10.1016/j.colsurfa.2008.12.035.

Martinez, A. C., Rio, E., Delon, G. et al. 2008. On the Origin of the Remarkable Stability of Aqueous Foams Stabilised by Nanoparticles: Link With Microscopic Surface Properties. *Soft Matter* **4** (7): 1531–1535. http://dx.doi.org/10.1039/B804177F.

Mo, D., Liu, N., Jia, B. et al. 2014. Study Nanoparticle-stabilized CO2 Foam for Oil Recovery at Different Pressure Temperature and Rock Samples. *Proc.*, SPE Improved Oil Recovery Symposium, Tulsa, Oklahoma, USA, 12–16 April. SPE-169110-MS. http://dx.doi.org/10.2118/169110-MS.

Mohanty, K. K. 2003. The Near-Term Energy Challenge. *AIChE J.* **49** (10): 2454–2460. http://dx.doi.org/10.1002/aic.690491002.

Nguyen, P., Fadaei, H., and Sinton, D. 2014. Nanoparticle Stabilized CO2 in Water Foam for Mobility Control in Enhanced Oil Recovery via Microfluidic Method. *Proc.*, SPE Heavy Oil Conference–Canada, Alberta, Canada, 10–12 June. SPE-170167-MS. http://dx.doi.org/10.2118/170167-MS.

Orr, F. M. 2007. *Theory of Gas-Injection Processes*. Copenhagen: Tie-Line Publications.

Orr Jr., F. M., Heller, J. P., and Taber, J. J. 1982. Carbon Dioxide Flooding for Enhanced Oil Recovery: Promise and Problems. *J. American Oil Chemists' Society* **59** (10): 810A–817A. http://dx.doi.org/10.1007/BF02634446.

Paul, K. T., Satpathy, S. K., Manna, I. et al. 2007. Preparation and Characterization of Nano Structured Materials From Fly Ash: A Waste From Thermal Power Stations, by High-Energy Ball Milling. *Nanoscale Research Letters* **2** (8): 397–404. http://dx.doi.org/10.1007/s11671-007-9074-4.

Rafati, R., Hamidi, H., and Idris, A. K. 2012. Application of Sustainable Foaming Agents to Control the Mobility of Carbon Dioxide in Enhanced Oil Recovery. Presented at the SPE Kuwait International Petroleum Conference and Exhibition, Kuwait City, Kuwait, 10–12 December. SPE-163287-MS. http://dx.doi.org/10.2118/163287-MS.

Roostapour, A. and Kam, S. 2013. Anomalous Foam-Fractional-Flow Solutions at High Injection Foam Quality. *SPE Res Eval & Eng* **16** (1): 40–50. SPE-152907-PA. http://dx.doi.org/10.2118/152907-PA.

Rossen, W. R. 1996. Foams in Enhanced Oil Recovery. In *Foams: Theory, Measurements, and Applications*, ed. Prudhomme R. K. and Khan S., Surfactant Science Series, 413–464. New York: Marcel Dekker.

Rossen, W., van Duijn, C., Nguyen, Q. et al. 2010. Injection Strategies To Overcome Gravity Segregation in Simultaneous Gas and Water Injection Into Homogeneous Reservoirs. *SPE J.* **15** (1): 76–90. SPE-99794-PA. http://dx.doi.org/10.2118/99794-PA.

Simjoo, M., Dong, Y., Andrianov, A. et al. 2013. Novel Insight Into Foam Mobility Control. *SPE J.* **18** (3): 416–427. SPE-163092-PA. http://dx.doi.org/10.2118/163092-PA.

Singh, R. and Mohanty, K. K. 2014. Synergistic Stabilization of Foams by a Mixture of Nanoparticles and Surfactants. *Proc.*, SPE Improved Oil Recovery Symposium, Tulsa, Oklahoma, USA, 12–16 April. SPE-169126-MS. http://dx.doi.org/10.2118/169126-MS.

Singh, R. and Mohanty, K. K. 2015. Synergy Between Nanoparticles and Surfactants in Stabilizing Foams for Oil Recovery. *Energy & Fuels* **29** (2): 467–479. http://dx.doi.org/10.1021/ef5015007

Spirov, P., Rudyk, S., and Khan, A. 2012. Foam Assisted WAG Snorre Revisit With New Foam Screening Model. Presented at the North Africa Technical Conference and Exhibition, Cairo, Egypt, 20–22 February. SPE-150829-MS. http://dx.doi.org/10.2118/150829-MS.

Stocco, A., Drenckhan, W., Rio, E. et al. 2009. Particle-Stabilised Foams: An Interfacial Study. *Soft Matter* **5** (11): 2215–2222. http://dx.doi.org/10.1039/B901180C.

Stocco, A., Rio, E., Binks, B. P. et al. 2011. Aqueous Foams Stabilized Solely by Particles. *Soft Matter* **7** (4): 1260–1267. http://dx.doi.org/10.1039/C0SM01290D.

Worthen, A., Bagaria, H., Chen, Y. et al. 2012. Nanoparticle Stabilized Carbon Dioxide in Water Foams for Enhanced Oil Recovery. *Proc.* SPE Improved Oil Recovery Symposium, Tulsa, Oklahoma, USA, 14–18 April. SPE-154285-MS. http://dx.doi.org/10.2118/154285-MS.

Worthen, A. J., Bryant, S. L., Huh, C. et al. 2013. Carbon Dioxide-in-Water Foams Stabilized With Nanoparticles and Surfactant Acting in Synergy. *AIChE J.* **59** (9): 3490–3501. http://dx.doi.org/10.1002/aic.14124.

Yu, J., Liu, N., Lee, R. L. et al. 2014. Study of Particle Structure and Hydrophobicity Effects on the Flow Behavior of Nanoparticle-Stabilized CO2 Foam in Porous Media. *Proc.*, SPE Improved Oil Recovery Symposium, Tulsa, Oklahoma, USA, 12–16 April. SPE-169047-MS. http://dx.doi.org/10.2118/169047-MS.

Robin Singh is a PhD degree candidate in the Center for Petroleum and Geosystems Engineering at the University of Texas at Austin. His research interests include nanotechnology and enhanced oil recovery (EOR). Singh holds a BTech degree in chemical engineering from Indian Institute of Technology, Kharagpur.

Kishore K. Mohanty is a professor of petroleum engineering and the director of the Center for Petroleum and Geosystems Engineering at the University of Texas at Austin. He worked at Arco Oil and Gas from 1981 to 1991 and taught at the University of Houston from 1991 to 2008. Mohanty's research is directed at EOR, formation evaluation, improved fracturing, and nanotechnology. He earned a BS degree from the Indian Institute of Technology, Kanpur, and a PhD degree from the University of Minnesota, both in chemical engineering. Mohanty received the 2008 Pioneer Award from the SPE Improved Oil Recovery Symposium and the 2013 SPE/AIME Anthony J. Lucas Gold Medal. He was the executive editor of *SPE Journal* during 2002–03.